

---

# Cytotoxicity of Some Indium Radiopharmaceuticals in Mouse Testes

Dandamudi V. Rao, Kandula S.R. Sastry, Hyranne E. Grimmond,  
Roger W. Howell, George F. Govelitz, Venkata K. Lanka, and Vijaya B. Mylavarapu

*Department of Radiology, University of Medicine and Dentistry of New Jersey, Newark, New Jersey and Department of Physics and Astronomy, University of Massachusetts, Amherst, Massachusetts*

The biological effects of [ $^{111}\text{In}$ ]oxine, [ $^{111}\text{In}$ ]citrate, and [ $^{114\text{m}}\text{In}$ ]citrate localized in mouse testes as well as the effects of external x-rays are investigated. The *in vivo* radiotoxicity of [ $^{111}\text{In}$ ]oxine is far greater than the chemotoxicity of oxine. Of these radiolabeled compounds, [ $^{111}\text{In}$ ]oxine is the most effective in reducing the sperm-head population, the mean lethal dose ( $D_{37}$ ) to the organ being about 0.16 Gy at 37% survival of the sperm heads. The corresponding values of  $D_{37}$  for [ $^{111}\text{In}$ ]citrate, [ $^{114\text{m}}\text{In}$ ]citrate and x-rays are  $\sim 0.34$ , 0.57, and 0.67 Gy, respectively. The present results affirm our earlier finding of the inadequacy of conventional dosimetry in estimating the biologic consequences of Auger-electron emitters *in vivo*. The very different radiotoxicities of [ $^{111}\text{In}$ ]oxine and [ $^{111}\text{In}$ ]citrate draw attention to the role of the chemical nature of the radiolabeled compounds in the expression of biologic effects *in vivo*, an aspect that is not considered explicitly in the formulation of conventional dosimetry.

J Nucl Med 29:375-384, 1988

---

Pharmaceuticals labeled with indium-111 ( $^{111}\text{In}$ ) are widely used as diagnostic agents in nuclear medicine. Recently, the biologic effects of this radionuclide have attracted attention (1-11). When lymphocytes from human peripheral blood were labeled with [ $^{111}\text{In}$ ]oxine, significant reduction of their proliferative capacity and severe chromosomal aberrations were reported (1). Neutrophil chemotaxis was noted in several experiments (2-6), while decreased colony forming ability was found by others (7-9) in some mammalian cell lines. There has been an interesting discussion over the reason for the observed biologic effects in the *in vitro* studies. Kassis and Adelstein (9) noted that the cytotoxic effects on Chinese hamster V79 lung fibroblasts, exposed to [ $^{111}\text{In}$ ]oxine, were due to the chemotoxicity of oxine, an avid metal ion chelator, present in the incubation medium. On the other hand, ten Berge et al. (1) suggested that the biologic damage to human lymphocytes in their work was the effect of radiations from the decay of  $^{111}\text{In}$  incorporated into the cells rather than the chemical, oxine. These differing views suggest the need for further studies (10-11).

The biologic consequences of  $^{111}\text{In}$  reported so far have been concerned with *in vitro* situations (1-9). The primary objective of this work is to investigate the *in vivo* effects of this radionuclide, which decays by electron capture (EC) and internal conversion (IC) in reaching the ground state of  $^{111}\text{Cd}$  (12). As in the cases of other radionuclides (e.g., iodine-125 ( $^{125}\text{I}$ ), thallium-201 ( $^{201}\text{Tl}$ ), iron-55 ( $^{55}\text{Fe}$ )) of biomedical interest (13-16), the EC and IC modes of decay lead to emission of several low energy electrons (Table 1) because of non-radioactive Auger and Coster-Kronig (CK) processes (15, 17,18) in the residual atom. By virtue of their subcellular ranges in biologic matter (Table 1), these electrons may irradiate the radiosensitive DNA effectively if  $^{111}\text{In}$  localizes in the nuclei of cells. Conventional dosimetry of tissue incorporated radionuclides (19-20), with its macroscopic considerations, ignores such effects. Because of this inadequacy, the biologic damage may be much more pronounced than expectations based on this approach.

We reported earlier that the Auger-electron emitters,  $^{201}\text{Tl}$  and  $^{55}\text{Fe}$ , when localized in the testes of mice, are about three times more efficient, per unit organ dose, in killing the spermatogonial cells than their beta emitting analogs,  $^{204}\text{Tl}$  and  $^{59}\text{Fe}$ , distributed similarly in the organ (13,16,21). In this work, we present the *in vivo* effects of intratesticularly (i.t.) administered [ $^{111}\text{In}$ ]oxine, [ $^{111}\text{In}$ ]citrate, and [ $^{114\text{m}}\text{In}$ ]citrate along with the

---

Received Feb. 2, 1987; revision accepted Aug. 10, 1987.

For reprints contact: Dandamudi V. Rao, PhD, Department of Radiology, University of Medicine and Dentistry of New Jersey, 100 Bergen Street, Newark, NJ 07103.

Theoretical Auger (A) and CK Electron Spectra Following the Decay of  $^{111}\text{In}$  and  $^{114\text{m}}\text{In}$ \*

No	Group	Yield per 100 decays	Average energy (keV)	Range ( $\mu\text{m}$ ) in unit density matter (34)
1	K <sub>A</sub>	14.4 (5.9)	20.1 (21.0)	9 (10)
2	L <sub>A</sub>	103 (69.4)	2.69 (2.8)	0.3 (0.3)
3	M <sub>A</sub>	208 (142)	0.351 (0.375)	0.017 (0.018)
4	L <sub>CK</sub>	14.9 (8.6)	0.182 (0.142)	0.008 (0.006)
5	M <sub>CK</sub>	92.5 (60.9)	0.124 (0.127)	0.005 (0.005)
6	N <sub>CK</sub>	254 (168)	0.039 (0.036)	0.002 (0.002)
7	N <sub>A</sub>	113 (83)	0.012 (0.017)	<0.001 (0.001)

\* The data for  $^{114\text{m}}\text{In}$  are given in parentheses.

effects of external irradiation of the testes by 60 and 120 kVp x-rays.

## EXPERIMENTAL DETAILS

### Experimental Approach

In these studies with indium radiopharmaceuticals, as in our earlier work (13,16,21,22), we have used spermatogenesis in mouse testes as the experimental model. The spermatogonial cells are very sensitive to radiation, whereas their precursors as well as the postgonial cells are relatively radioresistant (23, 24). This differential radiosensitivity provides the rationale for this model. The initial radiation damage to spermatogonia is expressed later as reduced sperm-head population when counted after the time necessary (4–6 wk) for spermatogonia to become spermatids. Besides its sensitivity to radiation effects (23,24), this model is also relevant to man (13,26–27). It is important that the survival of sperm heads is assayed on the day when their population in the testes attains its minimum value following initial exposure to ionizing radiation. This optimal day depends on the type of exposure and it should be determined experimentally in each case (13,24,25, 28).

Male Swiss Webster mice, 9–10 wk old and ~30 g each in weight, are employed. All radiolabeled and unlabeled compounds of interest are directly injected into the right testes of the animals following a minor surgical procedure. The i.t. mode of administration facilitates delineation of the in vivo effects of low-energy electrons (13,21).

### Radiopharmaceuticals

Indium-111 (Medi-Physics, South Plainfield, NJ) dissolved in ethanol was obtained at a specific concentration of 0.74 GBq/ml. This original stock contained oxine at a concentration of 1  $\mu\text{g}/\mu\text{l}$ . Carrier-free  $^{111}\text{In}$ chloride, and  $^{114\text{m}}\text{In}$ chloride (specific activity 0.11 GBq/mg) were obtained (Dupont Medical Products, No. Billerica, MA) in 0.05 N HCl solutions. The radioindium citrates were prepared following the proce-

dures of Sastry et al. (29). To 0.5 ml of a solution containing 15 mM sodium citrate and 150 mM sodium chloride, 20  $\mu\text{l}$  of the  $^{111}\text{InCl}_3$  stock was added to obtain  $^{111}\text{In}$ citrate at a pH of ~5.7. Signature for the  $^{111}\text{In}$ citrate complex was obtained through the physical technique of Perturbed Angular Correlation spectroscopy (29). Indium-114m citrate was prepared similarly.

### Methods

**General procedures.** These have been described in detail earlier (13,16,21,22). All the injected materials were contained in standard injection volumes (3  $\mu\text{l}$ ), the desired concentrations of the (radio) chemicals being realized through dilution in normal saline. Mice that were treated with i.t. injections of normal saline served as controls. Each data point obtained in these studies involved at least four or five mice, and the reproducibility was verified through several repetitions.

The first step is the study of biologic clearance of the radionuclides from the testes following their i.t. administration. Several mice were injected with 20 kBq of  $^{111}\text{In}$ oxine or  $^{111}\text{In}$ citrate, or 3.7 kBq of  $^{114\text{m}}\text{In}$ citrate. Groups of them were killed 0.25–144 hr later. The testes were removed, and the radioactivity remaining in the organ was assayed through gamma ray spectroscopy under standard geometry using a NaI detector with a 4-cm deep well, 1.75 cm in diameter, and a multichannel analyzer (Canberra, Model 10, Meriden, CT). The 171-keV and 245-keV gamma peaks in  $^{111}\text{In}$  decay (12) were integrated to determine the  $^{111}\text{In}$  activity in the samples relative to a precalibrated  $^{111}\text{In}$  standard. The  $^{114\text{m}}\text{In}$  activity was obtained by integrating over the 190 keV gamma peak (30). Clearance studies were also performed by injecting 10–20 times more radioactivity into the testes to ensure that the biologic elimination was not dependent on the injected dose.

The appropriate postinjection time for sperm-head survival assay is then established using mice, each receiving an initial i.t. injection of 1.1 MBq of  $^{111}\text{In}$ oxine or 1.3 MBq of  $^{111}\text{In}$ citrate. The animals were killed at different times, 12–45 days later. The testes were removed, homogenized in 1 ml of deionized water, sonicated for 30 sec, and the sperm heads, resistant to sonication, were counted in a hemocytometer under a microscope to a minimum of 200. These data (Figure 1) determine the postinjection time when the sperm-head population attains its minimum. Accordingly, mice injected with various doses of  $^{111}\text{In}$ oxine (0.093–2.2 MBq),  $^{111}\text{In}$ citrate (0.18–2.2 MBq), and  $^{114\text{m}}\text{In}$ citrate (3.7–74 kBq) were killed on the 36th day postinjection, and the fraction of surviving sperm heads, compared to controls, was determined.

As a standard protocol, checks were made (16) at different times to verify that the macroscopic distribution of the injected radionuclides is reasonably uniform over the testes. One day after i.t. injection of 0.55 MBq of  $^{111}\text{In}$ oxine, the mouse testes were processed for frozen section autoradiography (13). After one week of exposure, the grains were counted under a microscope in random sections and fields to assess the radionuclide distribution at the microscopic level. The distribution of the radionuclides in the cytoplasmic and nuclear fractions of cells in vivo is of value in understanding the experimental results. Mice were given i.t. injections of 0.37 MBq of  $^{111}\text{In}$ oxine (or  $^{111}\text{In}$ citrate), and the injected testes were removed at later times. Using the biochemical procedures described earlier (16), the testicular cells were isolated and separated into their cytoplasmic and nuclear fractions. The latter were

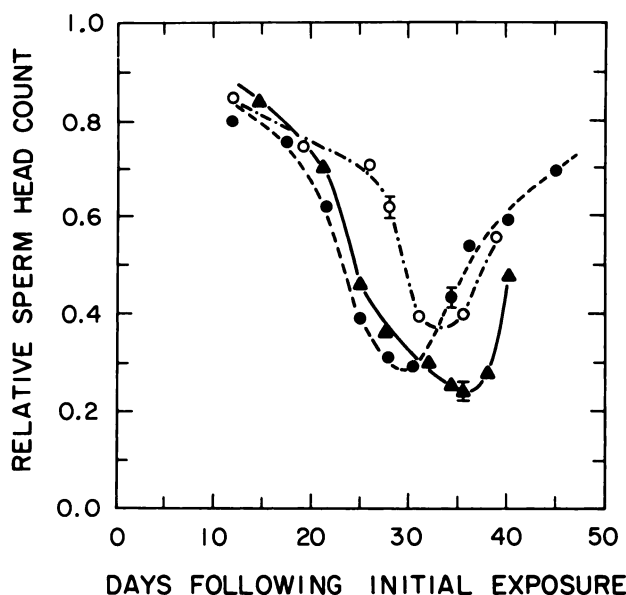


**FIGURE 1**

Time dependence of sperm-head population in mouse testes exposed to radiation. Relative sperm-head count is plotted as a function of the day of assay following initial i.t. injections of 1.1 MBq of [ $^{111}\text{In}$ ]oxine (solid triangles) or 1.3 MBq of [ $^{111}\text{In}$ ]citrate (open circles). The minimum is reached on the 36th and 34th day postinjection, respectively. The solid circles are data for external irradiation of the testes with constant doses (0.95 Gy) of 120 kVp x-rays, the minimum value occurring on the 29th day after the exposure. Representative uncertainties in the data (sdm) are shown. Minimum sperm-head count was also attained on the 29th day following i.t. injections of oxine (data not shown).

further separated into protein and DNA components. Aliquots of each were counted in the NaI well counter to obtain the intracellular radionuclide distribution.

**Irradiation by external x-rays.** The source of x-rays was an overhead fluoroscopy unit (GE Televi x 2, Schenectady, NY) (150 kVp). The effective photon energies of the beams produced at 60 and 120 kVp were 32 and 42 keV, respectively, determined by the "half value layer" method with aluminum absorbers. The field was uniform to within 3%. At these photon energies, the entrance dose will be somewhat higher than the dose at a depth of several millimeters of tissue. Experimentally, it is found that the effect of this is that the average exposure dose to testes is 96% of the entrance dose. During the testicular irradiation of the mice, the dose to the rest of the body was minimized by anesthetizing the animals with sodium pentobarbital (0.1 mg per 10 g of weight) and placing them in custom made lead shields, which exposed only the testes. The whole body protection thus provided was >99%. Thermoluminescent chips (3 mm  $\times$  3 mm  $\times$  1 mm, LiF) were placed in the center of the field for each exposure. These were processed in a commercial laboratory (Siemens Gamma Sonics, Inc., Des Plaines, IL). Fifty mice were given average testicular doses of 0.95 Gy each at 120 kVp to establish the postexposure time for attainment of minimum sperm-head population. This day was determined to be the 29th day postirradiation (Fig. 1). Mice exposed to testicular x-ray doses

in the range 0.02–1.0 Gy, both at 60 and 120 kVp, were assayed on this day for sperm-head survival.

**Chemical toxicity of oxine.** The observed effects of [ $^{111}\text{In}$ ]oxine on sperm-head survival are, in principle, a combination of the radiotoxic and chemotoxic effects on the spermatogonial cells. We investigated the effects of oxine so that the radiation effects of [ $^{111}\text{In}$ ] alone may be quantified. The various injection doses of [ $^{111}\text{In}$ ]oxine used in the sperm-head survival studies contained oxine in the range of 0.125–3.0  $\mu\text{g}$ . A stock solution of 8-hydroxyquinoline (Sigma Chemical Co., St. Louis, MO) (oxine) in ethanol was suitably diluted in normal saline so that the standard 3  $\mu\text{l}$  injection volumes contained the nonradioactive chemical in amounts ranging from 0.125–4.0  $\mu\text{g}$ . Following i.t. injections of this material into mice, the sperm-head survival was studied on the 36th day, when minimum sperm-head counts were observed with [ $^{111}\text{In}$ ]oxine.

Possible synergistic effects of radiation and the chemical were also studied. One hour after i.t. injection of 0.125–3.0  $\mu\text{g}$  of the chemical, the mice were given intraperitoneal injections of nembutal (1.8 mg 0.3 ml volume), and their testes were then exposed to various doses (0.02–0.4 Gy) of 120 kVp x-rays. Surviving sperm heads were counted on the 29th day after the exposure, when minimum sperm-head population was attained in the case of external x-rays, as well as with the chemical alone (see Fig. 1).

## RESULTS AND DISCUSSION

### Biologic Clearance

The patterns of biologic elimination (Figure 2) of [ $^{111}\text{In}$ ] and [ $^{114\text{m}}\text{In}$ ] from the testis, following i.t. administration of [ $^{111}\text{In}$ ]oxine, [ $^{111}\text{In}$ ]citrate, and [ $^{114\text{m}}\text{In}$ ]citrate, indicate a three-component clearance in the case of [ $^{111}\text{In}$ ] and two components for [ $^{114\text{m}}\text{In}$ ]. These data, including those taken at times later than 48 hr, were analyzed by the least squares method to obtain the relative weights of the various components ( $f_i$ ) and their biologic half-lives ( $T_{iB}$ ). The corresponding values of effective half-lives ( $T_{e}$ ) were calculated using the physical half-life of 2.83 days for [ $^{111}\text{In}$ ] (12) and 49.5 days for [ $^{114\text{m}}\text{In}$ ] (30). An interesting feature of these radio-pharmaceuticals is elimination of almost all of the radioactivity within minutes of injection in contrast with other radionuclides investigated by us (13,16,22). The significantly higher retention in the case of [ $^{114\text{m}}\text{In}$ ]citrate compared to [ $^{111}\text{In}$ ]citrate may be due to the fact that [ $^{114\text{m}}\text{In}$ ] is not carrier-free (Thakur ML, personal communication).

### Nuclear Radiations and Auger and CK Electron Spectra

Indium-111 and [ $^{114\text{m}}\text{In}$ ] decay schemes have been critically examined recently (12,30). Both radionuclides are Auger-electron emitters by virtue of their EC and IC modes of decay. The isomeric decay of [ $^{114\text{m}}\text{In}$ ] predominantly populates (95.7%) the 72s [ $^{114}\text{In}$ ], which decays almost entirely (99.5%) by emitting energetic beta rays. The Auger-electron spectrum for [ $^{111}\text{In}$ ] available in

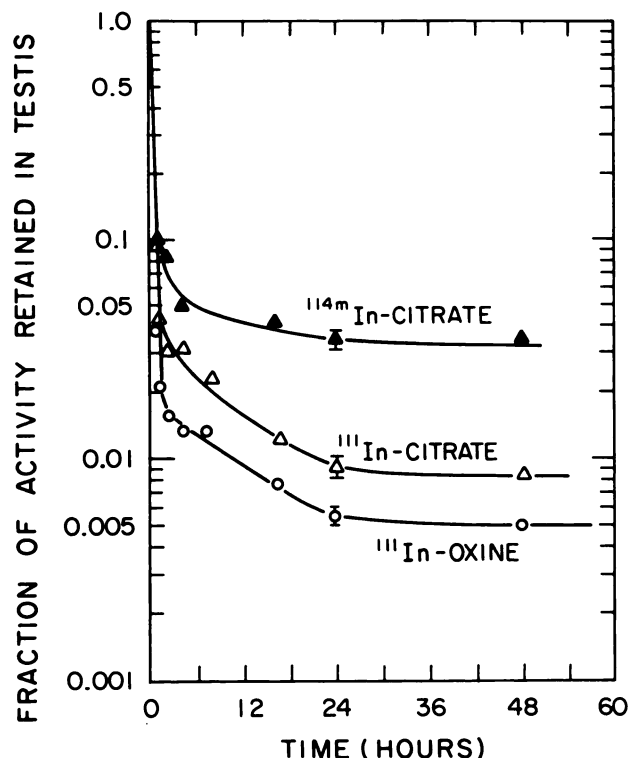


**FIGURE 2**  
Biologic elimination of indium radionuclides from mouse testes. Data are presented as semi-log plots of fraction of initially administered activity retained in the organ as a function of time. Data beyond the first 48 hr are not shown. The error bars indicate the standard deviation of the mean (sdm).

the literature (31) is incomplete in that important CK transitions and N shell Auger transitions were not taken into account, while the M shell Auger transitions were treated only approximately. There are no data on the Auger and CK electrons from  $^{114m}\text{In}$  decay. Therefore, we have calculated the spectra of nuclear radiations, atomic x-rays, and the Auger and CK electrons in the decay of both radionuclides using Monte Carlo methods (32) described in detail by Howell et al. (33). Besides the nuclear data on branching ratios, energy levels, and multipole nature of the transitions (12,30), we have used EC and IC subshell probabilities, atomic electron binding energies, and atomic x-ray, Auger, CK and super CK transition rates. References to these aspects may be found in recent papers (13-16,33). In these calculations, a total of 10,000 random decay events are considered for each radionuclide.

Table 1 is a brief summary of the complex Auger and CK electron spectra for both the radionuclides. Approximately eight such electrons are expected on the average per  $^{111}\text{In}$  decay compared to  $\sim 5$  per  $^{114m}\text{In}$  decay. These electrons have energies from about 10 keV-20 keV with ranges of  $\sim 1$  nm-10  $\mu\text{m}$  in biologically equivalent matter (34). The nuclear radiations

and atomic x-rays from the decay of these radionuclides are included in Table 2 for ready reference for dosimetric purposes.

#### Average Testicular Radiation Dose

The mouse testis has an average mass of 0.1 g, an essentially spherical shape, and an average radius of 2.9 mm for an organ of unit density. The absorbed fractions ( $\phi$ ) of various radiations emitted by  $^{111}\text{In}$  and  $^{114m}\text{In}$  in the testis are calculated for uniform distribution of the radionuclides in the organ. The methods employed to obtain these fractions for photons and beta rays have been described (13,16). For monoenergetic electrons, Eq. (2) of Ref. (35) is used. The fraction  $\phi$  is unity for L x-rays, and for the Auger and CK electrons; and it is 0.44 and 0.83, respectively, for the intense and weak beta groups in  $^{114m}\text{In}$ - $^{114}\text{In}$  decay. For the  $K_{\alpha}$  and  $K_{\beta}$  photons from  $^{111}\text{In}$  decay,  $\phi = 0.066$  and 0.045, respectively; the corresponding values for  $^{114m}\text{In}$  are 0.057 and 0.040. For the gamma photons,  $\phi$  ranges from 0.006-0.007. Values of  $\phi$  are between 0.94 and 0.98 for the IC electron groups. Using these results and the radiation data (Tables 1 and 2), the average energy ( $\epsilon$ ) deposited in the testis per  $^{111}\text{In}$  decay in the organ is calculated to be 37.0 keV, the electrons contributing an amount  $\epsilon_e = 33.2$  keV, 20% of which is from Auger electrons. The photon contribution,  $\epsilon_{ph}$ , is 3.8 keV. In the case of  $^{114m}\text{In}$ - $^{114}\text{In}$ ,  $\epsilon$  is 466 keV with  $\epsilon_{ph} = 1.2$  keV; and  $\epsilon_e = 464.8$  keV, the Auger electron contribution being 0.8%. These values of  $\epsilon$ , the data on  $f_j$  and  $T_{je}$  from the testicular clearance studies (Fig. 2), and Eq. (1) in Rao et al. (16) are used to calculate the average conventional organ doses. As noted before (16,22,24), the cumulated dose to the testis over the first 13-days

**TABLE 2**  
Nuclear Radiations and Atomic X-Rays in the Decay of  $^{111}\text{In}$  and  $^{114m}\text{In}$ - $^{114}\text{In}$

Radiation	$^{111}\text{In}$		$^{114m}\text{In} - ^{114}\text{In}^*$	
	Average energy (keV)	Yield per 100 decays	Ave. energy (keV)	Yield per 100 decays
$\gamma$	171.3	90.2	190.3	15.8
$\gamma$	245.4	94.1	558.4	4.4
$\gamma$	—	—	725.2	4.3
M x-Ray	Negligible	Negligible	Negligible	Negligible
L x-Ray	3.2	5.0	3.4	4.0
$K_{\alpha}$ x-Ray	23.1	69.4	24.1	31.0
$K_{\beta}$ x-Ray	26.2	14.2	27.2	6.1
IC electron	144.6	8.5	162.4	39.1
IC electron	168.1	1.3	187.2	40.7
IC electron	218.6	5.0	—	—
IC electron	241.9	0.9	—	—
Beta	—	—	777 <sup>†</sup>	95.1
Beta	—	—	222 <sup>‡</sup>	0.13

\* Parent and daughter in secular equilibrium.

<sup>†</sup> Maximum beta energy 1985 keV.

<sup>‡</sup> Maximum beta energy 686 keV.

postinjection period is the appropriate quantity in view of the long residence times of the radionuclides in the organ (Fig. 2). These 13-day cumulated testicular doses are 0.162, 0.226, and 16.5 Gy per MBq of initially injected [ $^{111}\text{In}$ ]oxine, [ $^{111}\text{In}$ ]citrate, and [ $^{114\text{m}}\text{In}$ ]citrate, respectively.

### Sperm-head Survival

**Optimal time for assay.** Figure 1 shows that the appropriate time for sperm-head survival assay is the 29th day following initial acute exposure of the testes to external x-rays, in agreement with the findings of Mian et al. (24,25) and expectations based on the time scale of events in spermatogenesis in mice (23,24). The corresponding time (Fig. 1) is the 36th day postinjection for [ $^{111}\text{In}$ ]oxine, and the 34th day for [ $^{111}\text{In}$ ]citrate and for [ $^{114\text{m}}\text{In}$ ]citrate (data not shown). These results are consistent with observations involving protracted irradiation of the testes by radionuclides with long residence times in the organ (16,21,22,24,28). In the case of the radioindium citrates, the relative sperm-head count is essentially the same on the 34th and 36th day within experimental uncertainties. It was therefore convenient to conduct sperm-head survival studies on the 36th day postinjection for all the three radiopharmaceuticals.

**Effects of x-rays.** The dose dependence of sperm-head survival (Fig. 3) is the same at 60 kVp and 120 kVp, the dose at 37% survival being  $0.67 \pm 0.03$  Gy. This

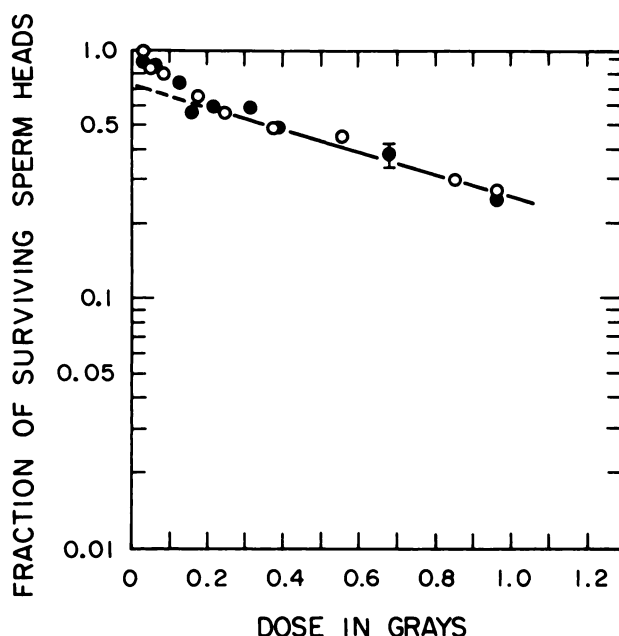


**FIGURE 3**

Sperm-head survival versus external x-ray dose to testes. Solid circles are the data with 60 kVp x-rays, and the open circles with 120 kVp x-rays. The survival fraction  $S$  is well represented by the function  $S = a_1 \exp(-D/D_{01}) + a_2 \exp(-D/D_{02})$  with  $a_1 = 0.28$ ,  $D_{01} = 0.08$  Gy; and  $a_2 = 0.72$ ,  $D_{02} = 1.0$  Gy. Typical uncertainty in data (sdm) is indicated.

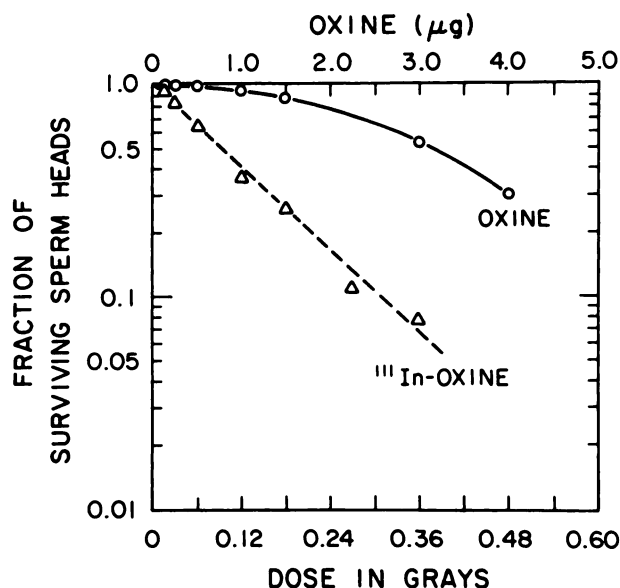


**FIGURE 4**

Effects of [ $^{111}\text{In}$ ]oxine and oxine on sperm-head survival. The surviving fraction of sperm heads in mice treated with i.t. injections of [ $^{111}\text{In}$ ]oxine or oxine is determined on the 36th day postinjection in comparison with the sperm-head count in the testes of unexposed animals. The [ $^{111}\text{In}$ ]oxine data, uncorrected for chemotoxic effects, are plotted against the average cumulated radiation dose to the organ from intratesticular [ $^{111}\text{In}$ ]. The data with oxine alone are presented as a function of the amount of the chemical injected (scale indicated at the top of the figure).

value compares favorably with the result of Mian et al. (25) using  $^{137}\text{Cs}$  gamma rays and  $\text{C}_3\text{Hf}/\text{BU}$  mice. The two-component nature of the dose response curve and the relative proportions of the two components are similar to our earlier findings with  $^{201}\text{Tl}$  (13) and  $^{55}\text{Fe}$  (16). This suggests that the shapes of sperm-head survival curves in our studies with the radionuclides in the testes (13,16) were real and not due to artifacts. The two components indicate two subgroups of spermatogonia with somewhat different average radiosensitivities in the testes of the strain of our mice. Comparable two-component spermatogonial cell survival curves have been recently reported by Gasinska (36) with 250 kVp x-rays and 5.5 MeV neutrons in a different strain of mice.

**Effects of indium-111-oxine in vivo: Radiation versus chemical toxicity.** In Figure 4, the effects of various injected doses of [ $^{111}\text{In}$ ]oxine (uncorrected for chemical effects) are compared with those of oxine. The drastic nature of reduction of the sperm-head population by [ $^{111}\text{In}$ ]oxine is in contrast with the gradual effects of oxine alone. At 1.0  $\mu\text{g}$  of injected oxine, chemical toxicity is barely noticeable, whereas the [ $^{111}\text{In}$ ]oxine dose (0.74 MBq) containing the same amount of cold oxine results in only about 37% sperm-head survival (Fig. 4). We note further that, with a 2.2 MBq [ $^{111}\text{In}$ ]oxine injection (0.36 Gy of testicular dose), the surviv-

ing fraction is reduced to 7.4%, while the equivalent amount of oxine (3  $\mu\text{g}$ ) results in a much higher (52%) survival (Fig. 4).

Does oxine sensitize the cells leading to enhanced radiation action? An answer is provided by our results on the sperm-head survival fractions with external x-rays ( $S_x$ ), with a combination of radiation and oxine ( $S_c$ ), and with oxine alone ( $S_o$ ), determined on the 29th day after the initial treatment. If there is no synergistic interaction between radiation and the chemical, the ratio  $R = S_c/S_o$  must be the same as  $S_x$ . That this is indeed the case is illustrated by three sets of data at different x-ray testicular doses ( $D$ ) and oxine amounts ( $M$ ):

- Set I.  $D = 0.40$  Gy,  $M = 3.0$   $\mu\text{g}$ ;  
 $S_c = 0.18$ ,  $S_o = 0.37$ ,  $R = 0.49$ ;  
 Set II.  $D = 0.29$  Gy,  $M = 2.5$   $\mu\text{g}$ ;  
 $S_c = 0.31$ ,  $S_o = 0.54$ ,  $R = 0.57$ ;  
 Set III.  $D = 0.15$  Gy,  $M = 1.0$   $\mu\text{g}$ ;  
 $S_c = 0.52$ ,  $S_o = 0.83$ ,  $R = 0.63$ .

From Figure 3,  $S_x = 0.48$ ,  $0.54$ , and  $0.65$  at the respective x-ray doses, in excellent comparison with the corresponding values of  $R$ .

**Sperm-head survival curves with the radioindium nuclides.** The above considerations permit us to derive the survival curve representing the radiation effects of  $^{111}\text{In}$  in  $^{111}\text{In}$ oxine by dividing the  $^{111}\text{In}$ oxine survival data (Fig. 4) by the corresponding values with oxine. Survival fractions thus obtained for  $^{111}\text{In}$  (oxine), and the sperm-head survival data with the radioindium citrates are presented in Figure 5 as a function of the conventionally calculated average dose to the organ. Clearly, the radionuclide effects of  $^{111}\text{In}$  (oxine) are more severe than the effects of the radioindium citrates.

The single-component nature of the survival curves (Fig. 5) is in contrast with the two-component responses observed in our earlier studies with intratesticularly localized radionuclides (13,16,22) and with external x-rays in this work (Fig. 3). Perhaps a more radioresistant second component might have revealed itself if the  $^{111}\text{In}$  data could be extended to higher doses. This was not possible, however, because of the limitation imposed by available initial radionuclide concentrations in the stock solutions. The apparent one-component nature of the  $^{111}\text{In}$  (oxine) curve might have been due to the effects of oxine. This is unlikely. X-ray exposure 1 hr after injection of oxine revealed no synergistic effects. Exposure to x-rays at subsequent times should not be expected to alter this conclusion in view of the fast clearance of the radionuclide (Fig. 2) and, presumably, the chemical as well (see Discussion). The  $^{114m}\text{In}$  data, extending to higher doses than with the  $^{111}\text{In}$  compounds, are also consistent with a single-component response. Thus, a second component, if any, should be relatively minor. A common feature of the three sur-

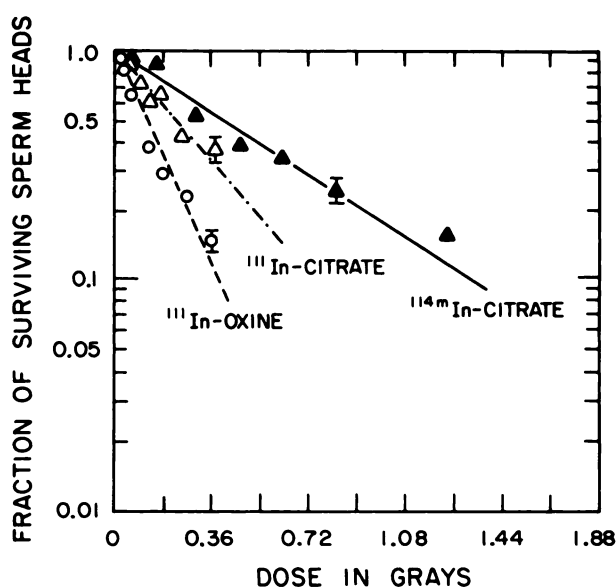


**FIGURE 5**  
 Sperm-head survival curves for  $^{111}\text{In}$ oxine,  $^{111}\text{In}$ citrate, and  $^{114m}\text{In}$ citrate. The data for  $^{111}\text{In}$ oxine are corrected for the relatively minor chemotoxicity of oxine. The abscissae give the conventionally calculated average radiation dose to the testis. Representative error bars (sdm) are shown.

vival curves in Figure 5 is that both  $^{111}\text{In}$  and  $^{114m}\text{In}$  emit Auger-electrons (Table 1), and the short-range effects of the low energy electrons could have had an influence on the shapes of the survival curves. However, this explanation may not be quite plausible since only a very small fraction of the dose is from Auger electrons from  $^{114m}\text{In}$ - $^{114}\text{In}$ . It is perhaps more likely that the different cell types included in the spermatid survival assay might have passed through a radiosensitive stage during the protracted exposure to the radionuclides.

#### Radionuclide Distribution

At times  $t \geq 12$  hr after i.t. administration, indium radioactivity per gram in the several frozen testicular sections was the same to within 10–15% of the average value per unit mass of the whole organ. This indicates that the organ is uniformly irradiated over this time scale at the macroscopic level. From the clearance data, we estimate that the bulk ( $\geq 60\%$ ) of the organ dose is delivered over  $t > 12$  hr. Microscopically,  $^{111}\text{In}$  is found in the tubular and intertubular spaces (Figure 6). Within the tubules, of 100  $\mu\text{m}$  diameter, the grains (radionuclides) are seen primarily in the basal 10  $\mu\text{m}$  layer of the seminiferous tubules containing the spermatogonia, Sertoli cells, and preleptotene and leptotene spermatocytes. Our intracellular distribution studies at different times show that  $\sim 92\%$  of  $^{111}\text{In}$  activity [ $^{111}\text{In}$ oxine) in the testicular cells is present in their nuclei and 8% in the cytoplasm. Of the nuclear content, 4% is found in



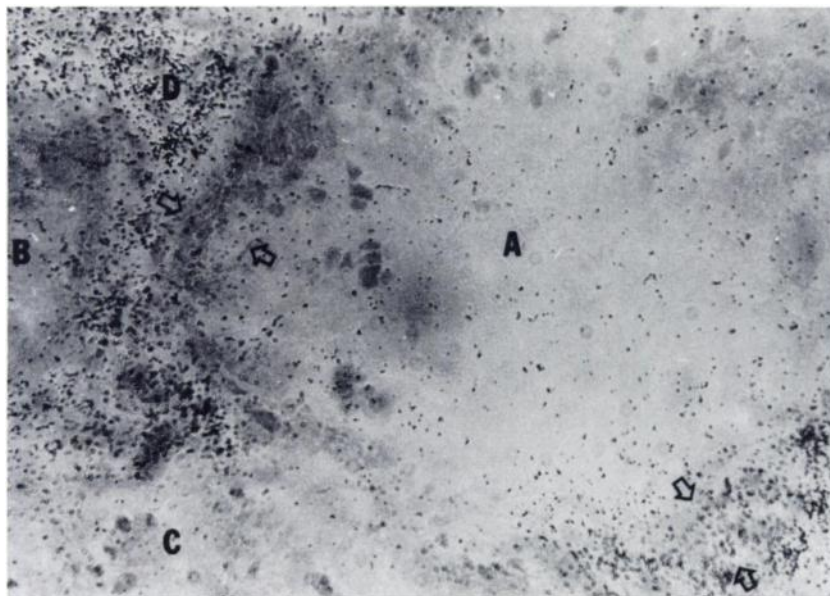


**FIGURE 6**

An autoradiogram of the seminiferous tubule of mouse testis 24 hr following i.t. injection of  $[^{111}\text{In}]$ oxine. The major part of a tubule (A), and minor parts (B,C) of two adjacent ones may be noted. Region D is intertubular space. The double arrows indicate the width of the basal  $10\ \mu\text{m}$  region of interest.

the DNA and the rest within the nucleoproteins. For the radioindium citrates, 70% of the cellular activity is in the cytoplasmic fraction and the rest in the nuclear fraction, 9% of which is in the DNA. In the cellular preparations, 10–15% of the cells were damaged (trypan blue test) resulting in their cytoplasm leaking out prior to the assay. The values quoted above were obtained after minor corrections (a few percent) of the raw data for this systematic effect.

#### Radiotoxicities

*Intercomparison.* It is customary to consider the mean lethal dose ( $D_{37}$ ) at 37% survival as an index of radiotoxicity. Least squares analysis of the survival data (Figure 5) gives the following values for  $D_{37}$ :  $0.16 \pm 0.01\ \text{Gy}$ ,  $0.34 \pm 0.03\ \text{Gy}$ , and  $0.57 \pm 0.05\ \text{Gy}$  for  $[^{111}\text{In}]$ oxine,  $[^{111}\text{In}]$ citrate, and  $[^{114m}\text{In}]$ citrate, respectively. At the time of i.t. administration, the  $^{111}\text{In}$  stock solution contained the long-lived  $^{114m}\text{In}$  as a 0.05% impurity of the total radioactivity (37). This results in a small enhancement (5%) of the doses calculated for pure  $^{111}\text{In}$  alone. This correction is included in the above values for  $^{111}\text{In}$  compounds. Our x-ray data (Fig. 3) give  $D_{37} = 0.67 \pm 0.03\ \text{Gy}$ . This indicates that the indium radionuclides are more effective in reducing the sperm-head population. Caution is needed, however, in any quantitative use of such comparisons because the biologic aspects are not quite the same in the two cases. The spermatid survival assay, 29 days after an acute x-ray exposure of the testes, reflects the effects on only one subgroup of the differentiating spermatogonia. In contrast, the indium radionuclides chronically irradiate the various subgroups of spermatogonia as they pass through different stages with changing radiosensitivities.

We have also studied the in vivo effects of beryllium-7 ( $^7\text{Be}$ ), which emits 477 keV gamma photons and only

a single Auger electron ( $\sim 40\ \text{eV}$ ) per decay (31). When introduced into the testis as  $[^7\text{Be}]\text{chloride}$ , 80% of the injected activity is very quickly eliminated and 20% stays in the organ with an effective half-life of 18 days. As a result, the spermatogonia are irradiated chronically and uniformly by the penetrating gamma rays. Interestingly, the sperm-head survival curve, its shape and the  $D_{37}$  dose for  $^7\text{Be}$  are the same as for external x-rays. Quantitative use of these results (to be presented elsewhere) should await further understanding of possible variables.

Amongst the indium radiocompounds,  $[^{114m}\text{In}]$ citrate is the least radiotoxic although it is similarly distributed in the cells as  $[^{111}\text{In}]$ citrate, and both the radionuclides are Auger-electron emitters. The  $^{114m}\text{In}$  decay is almost invariably followed by  $^{114}\text{In}$  decay with the emission of energetic beta rays of macroscopic ranges. Its relative inefficacy is not surprising considering that only 0.8% of the total dose stems from the Auger electrons, whereas the Auger electrons contribute 20% of the total dose in the case of  $[^{111}\text{In}]$ citrate.

Although the same radionuclide is involved,  $[^{111}\text{In}]$ oxine is about two times as radiotoxic as  $[^{111}\text{In}]$ citrate. This result can not be understood in terms of conventional macroscopic dosimetry (19–20) and points out the need for subcellular and microdosimetric considerations when Auger-electron emitters are involved.

*Microscopic considerations.* Biologic effects are expressed at the cellular level. Therefore, the radiation dose of consequence is not primarily the integrated average organ dose as presumed by conventional dosimetry (19–20), but the dose received by the nuclei of critical cells in the organ (13–16,26) containing the radiosensitive DNA. These considerations are receiving attention recently (13–16,38,39), especially in the case of Auger-electron emitters. The very short range of

action of the low energy electrons points to the role of cellular localization and subcellular distribution of Auger-electron emitters in relation to the DNA for an efficient induction of biologic effects (14-16,38-41).

Our experimental results with [ $^{111}\text{In}$ ]oxine and [ $^{111}\text{In}$ ]citrate indicate the importance of the above for in vivo situations. Using the method of Kassis et al. (41), we have calculated the energy deposited and the absorbed energy density in concentric spherical shells of unit density matter around the decay site of  $^{111}\text{In}$ . The results (Figure 7) show the prevalence of high density of absorbed energy in the proximity of the decay site, and suggest the need for submicroscopic dosimetry to understand the observed effects.

Kassis and Adelstein (9) found that V79 cells in culture concentrate  $^{111}\text{In}$  highly when exposed to  $^{111}\text{In}$ -oxine. Do the testicular cells concentrate  $^{111}\text{In}$  in vivo? Although autoradiography reveals grains in the 10  $\mu\text{m}$  basal layer of the seminiferous tubule, these results are not adequate to answer the question. Our subcellular distribution studies do reveal that 92% of [ $^{111}\text{In}$ ]oxine activity, and 30% of the [ $^{111}\text{In}$ ]citrate activity in the

testicular cells is present in the nuclear fractions. The differences stem from differences in the chemical nature of the compounds. The results pertain to all the testicular cells, and suggest the possibility that  $^{111}\text{In}$  subcellular distribution in the spermatogonial cells might be quite similar. In that event, the much higher nuclear content of [ $^{111}\text{In}$ ]oxine compared to [ $^{111}\text{In}$ ]citrate qualitatively accounts for the relative radiotoxicities of the two compounds.

## SUMMARY AND CONCLUSION

This work is a contribution to the area of biologic effects and dosimetry of Auger-electron emitters in vivo, aspects of interest to nuclear medicine and radiation protection but not yet well understood. We have studied the consequences of indium radionuclides of different radiation properties ([ $^{111}\text{In}$ ]citrate, [ $^{114\text{m}}\text{In}$ ]citrate) with the same chemical nature, and of different chemicals with the same radiation properties ([ $^{111}\text{In}$ ]oxine, [ $^{111}\text{In}$ ]citrate). We have found that the chemical effects of oxine in vivo are minor, and corrected for them quantitatively based on an investigation of the effects of the chemical and radiation. According to Thakur et al. (42), short exposure of cells to [ $^{111}\text{In}$ ]oxine is adequate for cell labeling. They also note that oxine is very quickly released from cells. In our work, over 98% of the injected [ $^{111}\text{In}$ ]oxine activity is cleared from the testis within minutes after i.t. injection (Fig. 2). The minimal nature of the chemotoxicity of oxine observed in our studies is presumably due to the fast clearance of oxine as well.

In this paper, we have presented complete Auger and CK electron spectra for  $^{111}\text{In}$  and  $^{114\text{m}}\text{In}$ . We have measured the distribution of the radionuclides in the testicular cells. The results may be compared with available in vitro studies. According to Goodwin (Ref. (43) p. 391), ~80% of  $^{111}\text{In}$  activity in blood cells labeled with [ $^{111}\text{In}$ ]oxine was found in their nuclei. Approximately 30% nuclear localization is reported for lymphocytes labeled with [ $^{111}\text{In}$ ]tropolone (44). That only a small fraction (3-4%) of the cellular activity is found in the DNA of testicular cells is consistent with the results of Thakur et al. (42) on blood cells.

The observed radiotoxicity of [ $^{111}\text{In}$ ]oxine relative to [ $^{111}\text{In}$ ]citrate correlates approximately with the relative nuclear content of  $^{111}\text{In}$  in the two cases. The present work confirms our earlier observations (13,16) regarding the inadequacy of conventional dosimetry (19-20) of Auger-electron emitters in vivo. Conventional dosimetry assumes uniform distribution of radionuclides in the organ and ignores their cellular localization and distribution, which, in turn, are determined by the chemical nature of the radiolabeled compounds. In this approach, one expects no difference between the effects

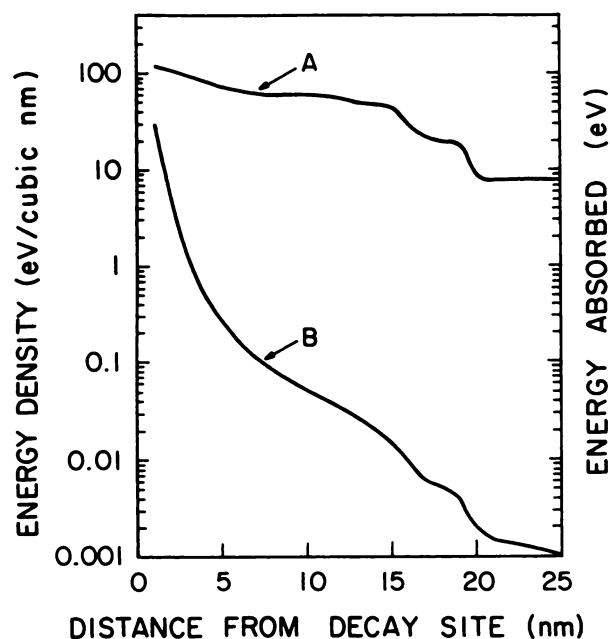


**FIGURE 7**  
Localized energy deposition around  $^{111}\text{In}$  decay site. Curve A shows the differential distribution of energy deposited by the Auger and CK electrons. The value at 1 nm is the energy absorbed in a unit density sphere of 1 nm radius, centered on the decay site. Thereafter, energy deposited in concentric spherical shells (1 nm thick) is shown as a function of the distance from the decay site. The discontinuities are due to the end of range effects of major low energy electron groups. Curve B, derived from the above, is the differential profile of average absorbed energy density. The drop of energy density by two orders of magnitude in the first 5 nm indicates the highly localized nature of the action of the low energy electrons. Note: 10 eV/(nm)<sup>3</sup> implies a local dose of 1.6 MGy.



of [ $^{111}\text{In}$ ]oxine and [ $^{111}\text{In}$ ]citrate. Our results to the contrary point out the limitation inherent in such an assumption.

Although  $^{114\text{m}}\text{In}$  is an Auger-electron emitter, there are no pronounced effects on sperm-head survival in this case, presumably because the cells are concurrently and efficiently irradiated by energetic IC electrons followed by the beta rays. Further studies on similar systems are needed to corroborate this finding of interest to dosimetry of incorporated radionuclides.

The radioindium pharmaceuticals used in this work as well as their i.t. administration may not be appropriate in human applications. Nevertheless, this basic research provides evidence for the effects of  $^{111}\text{In}$  in an in vivo model relevant to man. The radiotoxicity of  $^{111}\text{In}$  is intimately related to its localization in the cell nucleus. This emphasizes the need for intracellular distribution data for  $^{111}\text{In}$ -labeled radiopharmaceuticals in assessing the biologic implications. The value of such data with Auger-electron emitters in general has been recently noted (39).

## ACKNOWLEDGMENTS

The authors thank Doris Atkins for her help in the preparation of this manuscript, and Drs. M.L. Thakur and H. Huang for their interest and helpful comments. This work is supported by USPHS Grant CA 32877, and in part by a Research Corporation Grant. A preliminary report of some results of this work was presented elsewhere (45).

## REFERENCES

1. ten Berge RJM, Natarajan AT, Hardeman MR, et al. Labeling with  $^{111}\text{In}$  has detrimental effects on human lymphocytes: concise communication. *J Nucl Med* 1983; 24:615-620.
2. Segal AW, Deteix P, Garcia R, et al. Indium-111 labeling of leukocytes: a detrimental effect on neutrophil and lymphocyte function and an improved method of cell labeling. *J Nucl Med* 1978; 19:1238-1244.
3. Zakhirch B, Thakur ML, Malech HL, et al. Indium-111 labeled human polymorphonuclear leukocytes: Viability, random migration, chemotaxis, bactericidal capacity, and ultrastructure. *J Nucl Med* 1979; 20:741-747.
4. Burke JET, Roath S, Ackery D, et al. The comparison of 8-hydroxyquinoline, tropolone, and acetylacetone as mediators in the labeling of polymorphonuclear leukocytes with  $^{111}\text{In}$ : a functional study. *Eur J Nucl Med* 1982; 7:73-76.
5. Dettman GL, Iosiphidis AH. Functional integrity of mouse spleen lymphocytes in vitro after radiolabeling with  $^{111}\text{In}$ . *Radiat Res* 1982; 92:95-104.
6. Chisholm PM, Danpure HJ, Healey G, et al. Cell damage resulting from the labeling of rat lymphocytes and HeLa S3 cells with In-111 oxine. *J Nucl Med* 1979; 20:1308-1311.
7. Danpure HJ, Osman S, Hesslewood IP. Cell damage associated with [ $^{111}\text{In}$ ]oxine labeling of human tumor

- cell line (HeLa S3). *J Labelled Compd Radiopharm* 1979; 16:116-117.
8. Kraal G, Geldof AA. Radiotoxicity of indium-111. *J Immunol Methods* 1979; 31:193-195.
9. Kassis AI, Adelstein SJ. Chemotoxicity of indium-111 oxine in mammalian cells. *J Nucl Med* 1985; 26:187-190.
10. Watson EE. Cell labeling: radiation dose and effects. *J Nucl Med* 1983; 24:637-640.
11. Thakur ML, McAfee JG. The significance of chromosomal aberrations in indium-111-labeled lymphocytes. *J Nucl Med* 1984; 25:922-927.
12. Harmatz B. Nuclear data sheets for A=111. *Nuclear Data Sheets* 1979; 27:453-516.
13. Rao DV, Govelitz GF, Sastry KSR. Radiotoxicity of thallium-201 in mouse testes: inadequacy of conventional dosimetry. *J Nucl Med* 1983; 24:145-153.
14. Kassis AI, Adelstein SJ, Haydock C, et al. Thallium-201: An experimental and a theoretical radiobiological approach to dosimetry. *J Nucl Med* 1983; 24:1164-1174.
15. Sastry KSR, Rao DV. Dosimetry of low energy electrons. In: Rao DV, Chandra R, Graham M, eds. *Physics of nuclear medicine: recent advances*. New York: American Institute of Physics; 1984:169-208.
16. Rao DV, Sastry KSR, Govelitz GF, et al. In vivo effects of iron-55 and iron-59 on mouse testes: Biophysical dosimetry of Auger electrons. *J Nucl Med* 1985; 26:1456-1465.
17. Bambynek W, Crasemann B, Fink RW, et al. X-ray fluorescence yields, Auger and Coster-Kronig transition probabilities. *Rev Mod Phys* 1972; 44:716-813.
18. Hendee WR. Particulate radiations emitted during electron capture and isomeric transitions. *J Nucl Med* 1983; 24:1192-1193.
19. Loevinger R, Berman M. *A Revised Schema for Calculation of the Absorbed Dose from Biologically Distributed Radionuclides*. MIRD Pamphlet No. 1, revised. New York: Society of Nuclear Medicine; 1976.
20. ICRU Report 32. Methods of assessment of absorbed dose in clinical use of radionuclides. *International Commission on Radiation Units and Measurements* Washington, DC, 1979.
21. Rao DV, Sastry KSR, Govelitz GF, et al. Radiobiological effects of Auger electron emitters in vivo: spermatogenesis in mice as an experimental model. *Radiat Prot Dosim* 1985; 13:245-248.
22. Rao DV, Govelitz GF, Sastry KSR, et al. Spermatogonial cell killing by radiolabeled methionine: a comparative study of the effects of Se-75, S-35, and H-3. In: Schlafke-Stelson AT, Watson EE, eds. *Proceedings of the Fourth International Radiopharmaceutical Dosimetry Symposium*, CONF-851113. Oak Ridge Associated University, Oak Ridge, TN: International Radiopharmaceutical Dosimetry; 1986:52-66.
23. Meistrich ML, Hunter NR, Suzuki N, et al. Gradual regeneration of mouse testicular stem cells after exposure to ionizing radiation. *Radiat Res* 1978; 74:349-362.
24. Mian TA, Glenn HJ, Haynie TP, et al. Radiation dose effects on mouse testis from sodium P-32 phosphate: comparison with sodium Tc-99m-pertechnetate. In: Watson EE, Schlafke-Stelson AT, Coffey JL, et al., eds. *Third International Radiopharmaceutical Dosimetry Symposium*, HHS Publication FDA 81-8166. Washington, DC: U.S. Department of Health and Human Services; 1981:242-249.
25. Mian TA, Suzuki N, Glenn HJ, et al. Radiation dam-

- age to mouse testis cells from [ $^{99m}\text{Tc}$ ]pertechnetate. *J Nucl Med* 1977; 18:1116–1122.
26. Gaulden ME. "Biological dosimetry" of radionuclides and radiation hazards. *J Nucl Med* 1983; 24:160–164.
  27. Meistrich ML, Samuels RC. Reduction in sperm levels after testicular irradiation of the mouse: a comparison with man. *Radiat Res* 1985; 102:138–148.
  28. Mian TA, Glenn HJ, Haynie TP, et al. Radiation dose and biological effects to mouse testis from sodium P-32 phosphate. *Health Phys* 1982; 42:657–664.
  29. Sastry KSR, Hallee GJ, Ottlinger ME, et al. Some biophysical applications of perturbed gamma ray angular correlation. *Hyperfine Interactions* 1978; 4:891–906.
  30. Blachot J, Marguier G. Nuclear data sheets for A = 114. *Nuclear Data Sheets* 1982; 35:375–440.
  31. Dillman LT, Von der Lage PC. *Radionuclide Decay Schemes and Nuclear Parameters for Use in Radiation-Dose Estimation, MIRD Pamphlet No. 10*, New York: Society of Nuclear Medicine, Sept. 1975.
  32. Charlton DE, Booz J. A Monte Carlo treatment of the decay of  $^{125}\text{I}$ . *Radiat Res* 1981; 87:10–23.
  33. Howell RW, Sastry KSR, Hill HZ, et al. Cis-Platinum-193m: Its microdosimetry and potential for chemo-Auger combination therapy of cancer. In: Schlafke-Stelson AT, Watson EE, eds. *Proceedings of the Fourth International Radiopharmaceutical Dosimetry Symposium*, CONF-851113. Oak Ridge Associated University, Oak Ridge, TN: 1986:493–513.
  34. Cole A. Absorption of 20-eV to 50,000-eV electron beams in air and plastic. *Radiat Res* 1969; 38:7–33.
  35. Sastry KSR, Haydock C, Basha AM, et al. Electron dosimetry for radioimmunotherapy: Optimal electron energy. *Radiat Prot Dosim* 1985; 13:249–252.
  36. Gasinska A. Mouse testis weight loss and survival of differentiated spermatogonia following irradiation with 250 kVp X-rays and 5.5 MeV fast neutrons. *Neoplasma* 1985; 32:443–449.
  37. Marcus CS, Stabin MG, Watson EE, et al. Contribution of contaminant indium-114m/indium-114 to indium-111 oxine blood dosimetry. *J Nucl Med* 1985; 26:1091–1093.
  38. Adelstein SJ, Kassis AI, Sastry KSR. Cellular vs. organ approaches to dose estimates. In: Schlafke-Stelson AT, Watson EE, eds. *Proceedings of the Fourth International Radiopharmaceutical Dosimetry Symposium*, Oak Ridge Associated University, Oak Ridge, TN: CONF-851113. 1986: 13–25.
  39. Auger cascades and nuclear medicine. *The Lancet* 1985; 8454:533–534.
  40. Kassis AI, Sastry KSR, Adelstein SJ. Intracellular distribution and radiotoxicity of chromium-51 in mammalian cells: Auger-electron dosimetry. *J Nucl Med* 1985; 26:59–67.
  41. Kassis AI, Adelstein SJ, Haydock C, et al. Radiotoxicity of  $^{75}\text{Se}$  and  $^{35}\text{S}$ : theory and application to a cellular model. *Radiat Res* 1980; 84:407–425.
  42. Thakur ML, Segal AW, Louis L, et al. Indium-111-labeled cellular blood components: mechanism of labeling and intracellular location in human neutrophils. *J Nucl Med* 1977; 18:1020–1024.
  43. Hofer KG. Toxicity of radionuclides as a function of subcellular dose distribution. In: Watson EE, Schlafke-Stelson AT, Coffey JL, et al., eds. *Third International Radiopharmaceutical Dosimetry Symposium*, HHS Publication FDA 81-8166. Washington, DC: USHHS; 1981:371–391.
  44. Bandyopadhyay D, Levy LM, Das DK. Intracellular location of radionuclide in In-111 tropolone labelled polymorphonuclear leukocytes. *J Nucl Med* 1984; 25:98.
  45. Baverstock KF. Forum on microdosimetry of radiopharmaceuticals; committee on effects of ionising radiation. *Int J Radiat Biol* 1986; 50:555–568.